Halogenation of SiC for band-gap engineering and excitonic functionalization

L. B. Drissi[1,2], F. Z. Ramadan[1], S. Lounis[3,*]

[1] *LPHE, Modeling & Simulations, Faculty of Science, Mohammed V University in Rabat, Morocco*

[2] *CPM, Centre of Physics and Mathematics, Faculty of Science, Mohammed V University in Rabat, Morocco and*

[3] *Peter Grünberg Institut and Institute for Advanced Simulation, Forschungszentrum Jülich and JARA, D-52425 Jülich, Germany.*

Abstract

The optical excitation spectra and excitonic resonances are investigated in systematically functionalized SiC with Fluorine and/or Chlorine utilizing density functional theory in combination with many-body perturbation theory. The latter is required for a realistic description of the energy band-gaps as well as for the theoretical realization of excitons. Structural, electronic and optical properties are scrutinized and show the high stability of the predicted two-dimensional materials. Their realization in laboratory is thus possible. Huge band-gaps of the order of 4 eV are found in the so-called GW approximation, with the occurrence of bright excitons, optically active in the four investigated materials. Their binding energies vary from 0.9 eV to 1.75 eV depending on the decoration choice and in one case, a dark exciton is foreseen to exist in the fully chlorinated SiC. The wide variety of opto-electronic properties suggest halogenated SiC as interesting materials with potential not only for solar cell applications, anti-reflection coatings or high-reflective systems but also for a possible realization of excitonic Bose-Einstein condensation.

Keywords: SiC hybrid; Halogenation; GW approximation; electronic and optical properties; excitonic effects.

I. INTRODUCTION

Graphene has been largely studied and developed as a promising candidate for both fundamental research and advances in nanotechnology. This carbon nanosheet carries many unique properties over conventional materials such as high electrical conductivity, high electron mobility at room temperature [1, 2], and excellent optical transmittance [3] in the visible light range, which render this material highly promising for transparent conducting electrodes [4] and solar cells [5]. Moreover, transparent electrode based-graphene yields white organic light-emitting diodes with brightness and efficiency sufficient for general lighting [6].

Functionalization of graphene in order to tune its properties by different combinations of several types of materials is a large stream of activities in what we would name graphinology. For instance, oxygenation[7] and hydrogenation [8] has inspired intense search for novel graphene-based materials. Fluorographene and chlorographene, engineered under ambient conditions [9, 10], are highly stable thanks to the large electronegativity of fluorine and chlorine adsorbates [11]. Interestingly, in graphene halides, the binding of F- and Cl-atoms to the graphene surface leads to covalent bonds that change the hybridization state from sp^2 to sp^3 [12]. However, carbon orbitals retain their sp^2 hybridization during the adsorption of bromine and iodine. A crucial impact of halogens is in significantly decreasing the gap energy of their hydrogenated counterparts, making the new derivatives suitable for channel materials [11]. Interestingly, diatomic halogen molecules (I_2, Br_2) change carrier concentration in graphene without significant reduction of their mobility near the Dirac point [13]. Fully co-decorated graphene sheets with chemical species such as HF and HCl were also reported [14]. The resulting structures present a low level of disorder, high stability and band-gaps of about 3eV. Many of these properties are shared with 2D counterparts of graphene, such as silicene halides (see e.g. [15–18]). Interestingly, effective carrier masses in the latter complex are comparable in certain directions to those of silicon and show a relatively high mobility [19].

Our investigation is related to a relatively new 2D material, SiC, based on graphene and silicene, so-called silicene-graphene, which has been recently synthesized [20], following theoretical predictions [21]-[24]. SiC offers an alternative to overcome limitations associated with graphene electronic technologies. For example, it has a non-zero direct band gap energy with a high exciton binding energy E_b of $0.81eV$ as predicted by theory using GW built from localized density approximation- [25]. The gap opening originates from the alternated arrangement of carbon and

silicon in a two-dimensional honeycomb lattice which breaks the sublattice symmetry (see e.g. [23]). Thus, SiC hybrid could also be a remarkable candidate for novel type of light-emitting diodes as it shows improved photo-luminescence compared to its sphalerite or wurtzite counterparts [26].

Our interest is focused further on the ability to engineer excitons, which in nanostructures can have large binding energies. These excited quasi-particles (QP) made of an electron bound to a hole are pivotal in optoelectronic and thus, in photovoltaics, photoluminescence (see e.g. [27]) and potentially even in quantum information technology [28]. Excitons can be of the bright-type, i.e. optically active and thus of strong interest, or of the dark-type, i.e. optically inactive. The difference between the two types of excitons hinges on the spin-alignment of the electron and of the hole. However as highlighted by Poem et al.[28], dark excitons could also be of use in opto-applications directed towards quantum information technology.

Contrary to graphene and silicene, less attention has been devoted to functionalization of 2D-SiC with atomic decoration. Interestingly, full hydrogenation of SiC, where H-atoms passivate the surface via the unpaired electrons of the substrate atoms, yields to a buckled system with an insulating character [23]. The new material was predicted to be mechanically stable with strong resistance to the in-plane strains and shear waves can propagate faster than graphene along a specific direction [29]. Partial hydrogenation, however, has the opposite effect on the electronic structure since the gap is reduced in favor of ferromagnetism [23]. Similar to hydrogenation, complete fluorination tailors electronic properties of SiC and semi-fluorination has the additional advantage to induce novel magnetoelectric properties [30].

The goal of our work is to provide a first-principles based investigation of opto-electronic properties of 2D-SiC functionalized through halogenation. The latter allows tuning the band gap together with a generation of excitons having a high binding energy. Atomic decoration is made with either F, Cl or a combination of both elements. For an accurate quantitative estimation of gap energies of 2D materials required for practical applications, it is essential to utilize many-body perturbation theory within GW approximation that goes beyond the usual approximations LDA and GGA [31, 32]. Many-body effects, such as e-e correlations, included in the GW approximation correct the optical response, while e–h interactions as described in the framework of the Bethe-Salpeter equation (BSE) are required for the excitonic effects [33].

We consider four configurations: (i) full fluorinated silicene/graphene hybrid (F-SiC-F), (ii) full chlorinated hybrid (Cl-SiC-Cl), (iii) mixed Cl-SiC-F where F-atom decorate the carbon atoms

while Cl-atom the silicon atoms and (iv) the opposite mixed configuration F-SiC-Cl. Phonon frequencies analysis reveals the stability of all conformers. Our calculations demonstrate that halogen-atoms can greatly enhance excitonic effects in silicene/graphene hybrid, where the binding energies of the four configurations are higher than of pristine. The highest exciton binding energy of 1.75eV is found in F-SiC-Cl. We recall that bound excitons in fluorographene have a large formation energy, 1.96eV, of bound excitons [34] compared to 1.25eV obtained for chlorographene [35], while in fluorinated silicene, the binding energy is of 1.48eV [36]. The reflectivity spectra demonstrate that these materials are transparent in the visible region.

II. COMPUTATIONAL DETAILS

To study phonon spectra, structural, electronic and optical properties of halogenated SiC, we use the Quantum espresso (QE) simulation package [37] based on DFT and employing the GGA functional of Perdew-Burke-Ernzerhof (PBE) [38]. A norm-conserving pseudo-potential description [39] is used. A kinetic energy cutoff of 65Ry was applied for the plane-wave basis. In the Monkhorst-Pack grid, the Brillouin-zone integration was carried out at $16 \times 16 \times 1$ k-points for describing the band structure while the stabilities of structures are examined by calculating binding and formation energies and performing phonon dispersions using $20 \times 20 \times 1$ k-points. The optimized unit cell is obtained by minimizing the total energy as a function of the lattice parameter. All the structures are relaxed using a criterion of forces and stresses on atoms; until the energy change is smaller less than 10^{-4}eV.

The energy band gap is corrected using non-self consistent GW calculations implemented in YAMBO program suite [40]. In the GW approximation, the exchange-correlation potential V_{xc} used in the DFT is replaced by a nonlocal, energy-dependent self-energy operator. The first order quasiparticle (QP) corrections are obtained using Hedin [41] GW approximation, while excitonic effects are treated by solving the Bethe-Salpeter equation (BSE) [33]. In our calculations of QP energies, we use a $12 \times 12 \times 1$ k-point mesh. The same mesh is used to evaluate the dielectric function in both the random phase approximation (RPA) [42] and in the Tamm-Dancoff approximation [43] that considers only the resonant part of the BSE.

The charges of the ions were calculated according to Bader formalism that gives the charge of each atom constituting the material by integrating over the gradient paths of its electronic density [44].

III. RESULTS AND DISCUSSION

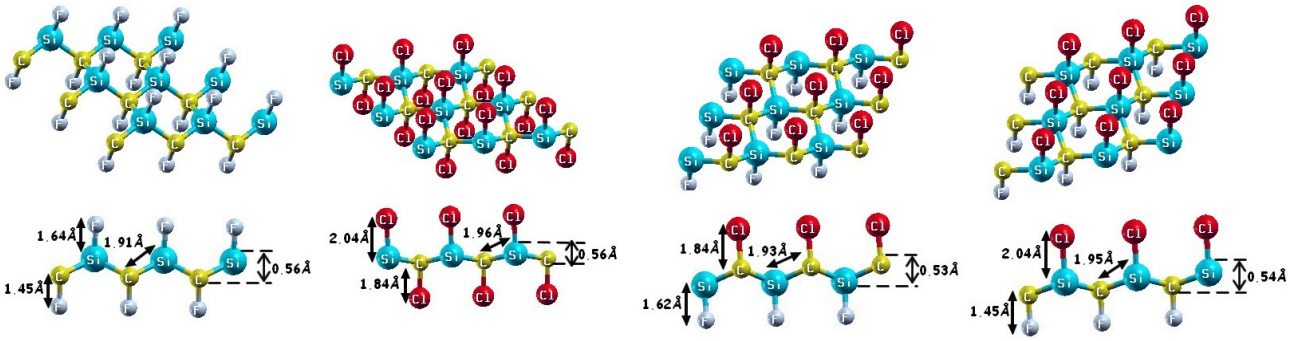

FIG. 1: Top and side views of the fully relaxed structures showing interatomic distances.

Silicene-graphene hybrid is stable in a planar hexagonal lattice with all bond angles $Si\widehat{C}Si$ and $C\widehat{Si}C$ equal to 120°. The bond length C-Si of 1.78$\mathring{A}$ is bounded below by the one of graphene and above by the one of silicene [21, 23]. In the following, we study full halogenated SiC where all the species adopt a chair configuration because it is the most stable one with respect to zigzag, boat and armchairs [18, 35].

Four structures in chair configuration, namely F-SiC-F, F-SiC-Cl, Cl-SiC-F and Cl-SiC-Cl, are considered. As shown in Fig.1, full fluorinated (chlorinated) SiC referred as F-SiC-F (Cl-SiC-Cl), are obtained by attaching F (Cl) atoms to C atoms in one side and to Si atoms in the opposite side of the plane. In chlorosilicene-fluorographene hybrid, Cl-SiC-F, all carbon atoms are decorated by fluorine atoms and all Si atoms bond chlorine atoms forming 1up/1down fashion on either side of the sheet. In F-SiC-Cl, the role of coadsorbed F- and Cl-atoms are inverted.

Structure parameters, listed in Table 1, reveal that both C- and Si-atoms are displaced along the normal direction from the plane of SiC layer as they are fourfold coordinated and form sp^3 hybridization with their neighbors. As a consequence, the halogenated structures are buckled and their bonds Si–C are stretched, ranging in between 7% and 10%, with respect to pure SiC hybrid. The interatomic distances $d_{\mathrm{F-C}}/d_{\mathrm{Cl-C}}$ and $d_{\mathrm{F-Si}}/d_{\mathrm{Cl-Si}}$, that increase with the increase of the atomic number of halogen elements, are in line with data calculated for halogenated graphene [11] and halogenated silicene [18].

Relative stability of configurations is studied first by evaluating their binding E_B and formation E_F energies with respect to the energies of pure SiC and of the isolated molecules made of the

Formers	d_{Si-C}	d_{Si-ad}	d_{C-ad}	Δ	E_B	E_F	E_{gap}^{GGA}	E_{gap}^{GW}	E_b^{e-h}	M_{eff}	r_{Bohr}
Pure	1.78	-	-	0.00	-	-	2.52	3.53	1.05	0.53	2.14
F-SiC-F	1.91	1.64	1.45	0.56	−2.32	−1.45	1.87	4.47	1.74	0.40	2.34
F-SiC-Cl	1.93	1.62	1.84	0.53	−1.93	−1.05	1.89	4.71	1.75	0.40	2.24
Cl-SiC-F	1.95	2.04	1.45	0.54	−1.71	−0.83	2.05	4.26	0.9	0.22	4.40
Cl-SiC-Cl	1.96	2.04	1.84	0.57	−1.33	−0.44	2.25	4.38	1.31	0.26	3.36

TABLE I: Structural parameters and different energies characterizing the pure and the four types of decorated SiC. The interatomic distances d, the buckling parameter Δ and Bohr radius, r_{Bohr}, are given in $\AA$. The Binding energy E_B, formation energy E_F, gap energy E_{gap} and excitonic binding E_b^{e-h} energies are all in eV while the effective mass of the exciton, M_{eff}, is given in terms of the bare electron mass m_0.

adsorbate. The corresponding energies are expressed as [45]:

$$E_B = \frac{1}{N}\left[E_T - E_{\text{SiC}} - n_{\text{ad}}E_{\text{ad}}\right] \quad \text{and} \quad E_F = \frac{1}{N}\left[E_T - E_{\text{SiC}} - \frac{1}{2}\left(n_{\text{ad}}E_{\text{ad}_2}\right)\right] \tag{1}$$

where N is the total number of atoms per unit cell, E_T is the total energy of the (co)-decorated structure and E_{SiC} is the energy of pristine SiC, n_{ad} is the number of adsorbated atoms in the supercell under consideration, E_{ad} and E_{ad_2} describe respectively the energy of an isolated adsorbed atom and the energy of the corresponding molecule.

Data in Table 1 shows that all configurations have negative formation and binding energies. Therefore, the structures are stable and the adsorptions are exothermic processes that could then be synthesized in experiments. Fluorine adsorbed on SiC sheet generates the most stable structure among halogen adsorbates. This result is in good agreement with previous works on halogenated graphene and halogenated silicene [18, 35].

Fig.2 displays dispersions of phonon modes, which is a reliable test for the examination of thermodynamic stability of halogenated SiC hybrids. The analysis of the curves shows that all phonon branches do not have imaginary frequency along any high-symmetry direction of the Brillouin zone. This is a signature of stability of the four structures. Each phonon spectrum includes 12 phonon bands, 3 acoustic and 9 optical. Phonon frequencies soften monotonically from full fluorinated to full chlorinated SiC due to the increasing atomic weight. It is observed that acoustic and optical branches are separated by a band gap in F-SiC-F. As a result, it is rather difficult to satisfy the energy conservation law during the phonon-phonon scattering between acoustic and optical modes in this structure.

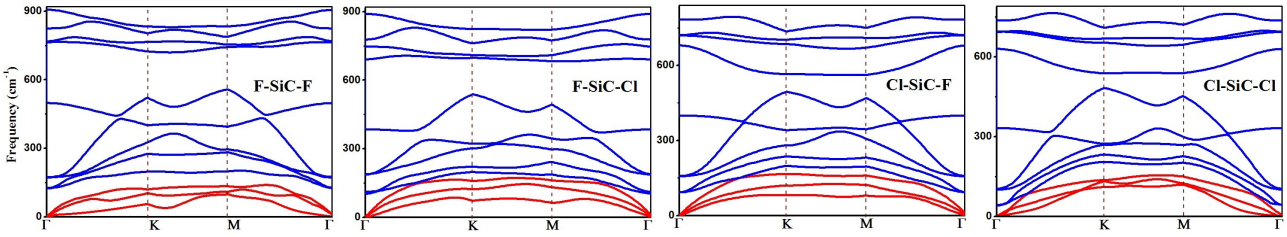

FIG. 2: Frequencies of the phonon modes of halogenated SiC hybrids. The optical branches are shown in red while the acoustical ones are in blue.

	F-SiC-F	Cl-SiC-Cl	F-SiC-Cl	Cl-SiC-F
C	−0.96	−0.96	−0.96	−0.97
Si	+3.86	+3.85	+3.85	+3.88
$ad_{/C}$	−0.69	−0.20	−0.14	−0.72
$ad_{/Si}$	−0.98	−0.97	−0.97	−0.97

TABLE II: Charge transfer involved in the four studied compounds: (+) sign denotes loss of electrons in opposite to (-) sign.

To grasp the bonding nature among atoms, Table 2 summarizes values of charge transfer for the four species calculated using Bader charge analysis. C-atoms are charge acceptors with $\sim 0.96e$ obtained from their Si-surroundings. It follows that the bond between Si and C is ionic. Moreover, the adsorbates gain an important amount of charge from their Si-atoms neighbor compared to the smaller electrons density transferred from C-atoms. This behavior can be attributed to Pauling electronegativities of F (3.98), Cl (3.16), C (2.55) and Si (1.9), since electrons are pulled away from atoms having lower electronegativity towards atoms with a higher one. Except C-Cl that forms a covalent bond, all the other bonds in the four configurations are ionic, which makes them suitable for many applications, because ionic materials are strong, hard and also they have a high melting point.

Electronic band structures displayed in Fig.3 and their corresponding gap energies given in Table 1 are calculated employing two different theoretical approaches. Standard GGA-DFT formalism reveals that all the structures are semi-conductors with a direct gap located at the Γ point in the Brillouin zone. The highest gap is found for Cl-SiC-Cl followed by Cl-SiC-F. The structures F-SiC-Cl and F-SiC-F have smaller gap energies. After quasi-particle corrections using the GW approximation, which is known to improve the gap description, the band gap becomes indirect

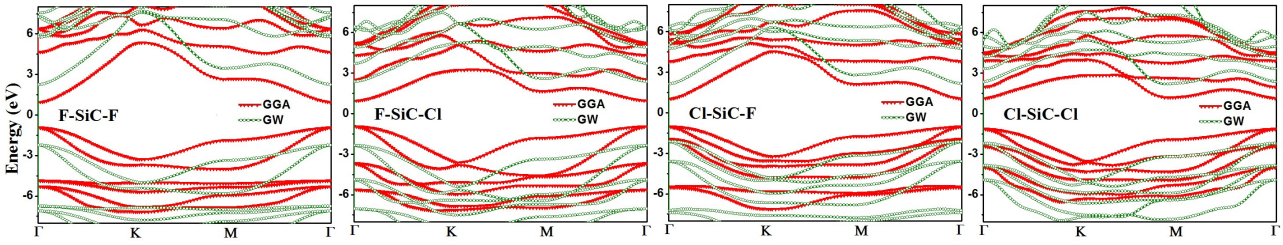

FIG. 3: Band structures in Brillouin zone. Red solid squares and green circles correspond to GGA and GW respectively. Energy is given with respect to the Fermi energy.

between Γ and M points in Cl-SiC-Cl conformer while it remains direct at Γ in the three other configurations. The values of band gap obtained from GW are much larger than those obtained from GGA. Moreover, the increasing sequence of the band gaps is completely inverted in comparison to the GGA derived values since F-SiC-Cl and F-SiC-F have the highest gap energies of 4.71eV and 4.47eV respectively followed by Cl-SiC-Cl and finally Cl-SiC-F.

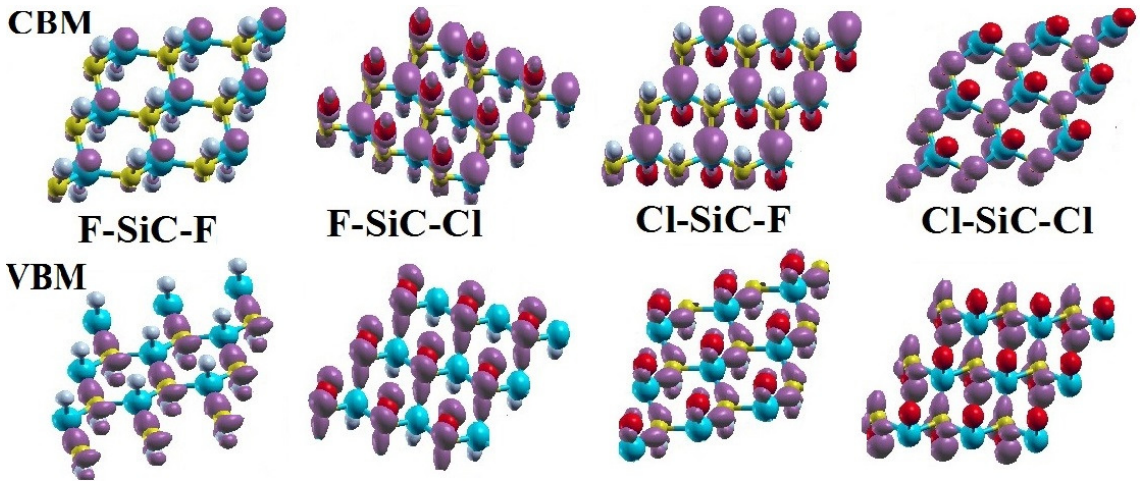

FIG. 4: Isosurface charge densities plots describing CBM (upper) and VBM (lower) corresponding to the four derivatives. The contour isovalue is set at 40%.

To gain further insights into the gaps character, partial density of states (PDOS) and charge distribution describing the lowest conduction band (CBM) and the highest valence band (VBM) are plotted. A first analysis of Fig.4 indicates that CBM mainly originates from orbitals of C and Si atoms, while orbitals of halogen atoms contribute also to VBM. More precisely, the PDOS of the four structures (see Fig.5) shows that the lower energy of CBM is dominated by p-electrons of Si-atoms followed by C-atoms. However, the situation is quite different in VBM. Indeed, in F-SiC-F, VBM is formed by p-orbitals corresponding to C-atoms, Si-atoms and fluorine that decorates

C-atoms (referred as $F_{/C}$-atoms). In Cl-SiC-Cl, both p-orbitals of C-atoms and Cl that bond C-atoms (referred as $Cl_{/C}$) contribute in VBM. In F-SiC-Cl, VBM consists mainly of Cl/C p-orbitals followed by less involving of C-atoms. Finally, in Cl-SiC-F, VBM is mainly composed of p-electrons of C- and Cl-atoms that are attached to Si (referred as $Cl_{/Si}$).

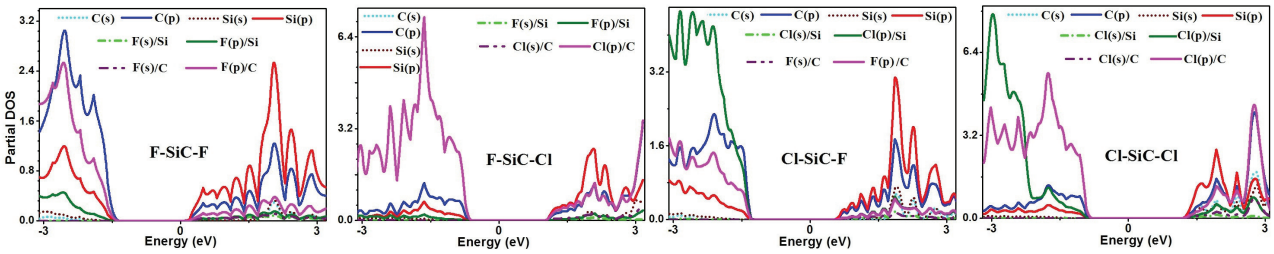

FIG. 5: Projected density of states corresponding to s- and p-orbitals of atoms composing the hybrids. The energy is given with respect to the Fermi energy.

In Fig.6 optical absorption spectra are depicted for light polarization along and perpendicular to halogenated SiC sheets. Local field effects (LFE) are also considered using GGA and the Random Phase Approximation (RPA). Similar to graphene [32] and pure GeC monolayer [46], when light polarization is in-plane, LFE have no significant influence on the species except a very slight reduction in their intensities. However, effects of local field are more important for out-of-plane polarization. In this case, LFE shift optical absorption's curves to higher frequencies and reduce significantly the spectrum intensity in the four structures. Moreover, in presence of the local field, the halogenated hybrids F-SiC-F, F-SiC-Cl, Cl-SiC-F and Cl-SiC-Cl are transparent below 2.04eV, 2.52eV, 2.24eV and 3.44eV respectively.

Optical absorption spectra are determined by the imaginary part of the macroscopic dielectric function, $Im\,[\varepsilon(\omega)]$. In the absence of LFE, Fig.7 displays $Im\,[\varepsilon(\omega)]$ calculated either without electron–hole interaction (GW-RPA) or including excitonic effects from the solution of Bethe–Salpeter equation (BSE). Only incident light polarized along x–direction is considered. The effective mass M_{eff} of the bright exciton is given by the expression [47]:

$$M_{eff} = \frac{E_b^{e-h}}{R_H}\varepsilon_r^2 m_0, \tag{2}$$

where R_H is the Rydberg energy, ε_r is the dielectric constant, m_0 is the electron rest mass and E_b^{e-h} is the excitonic binding energy. The Bohr radius of this core exciton can also be calculated with the following equation [47]

$$a = \frac{\varepsilon_r}{M_{eff}} a_H m_0, \tag{3}$$

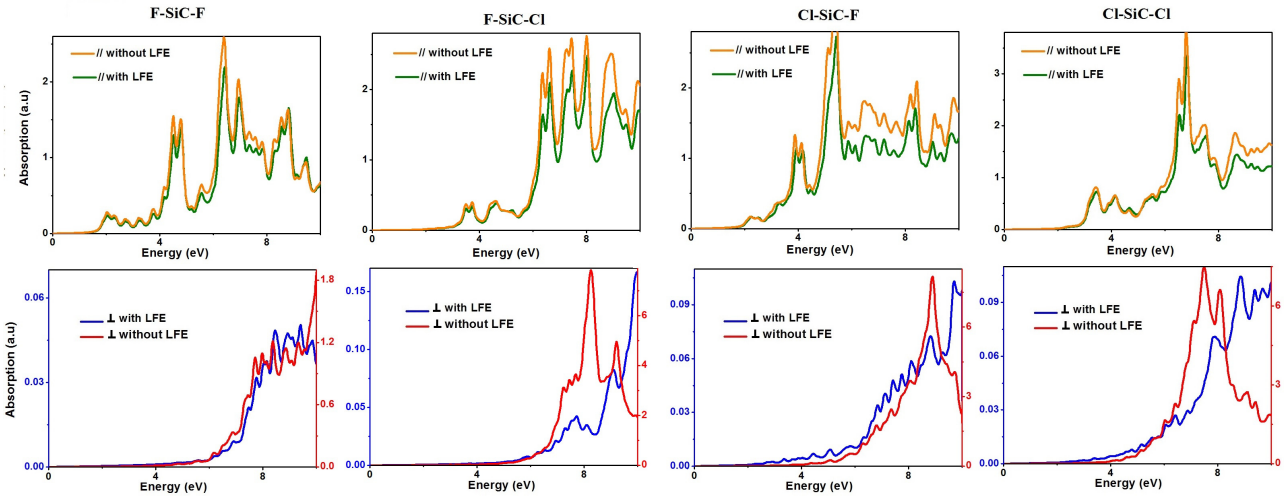

FIG. 6: Local field effects (LFE) on optical absorption spectra for light polarized (top figures) parallel and (down figures) perpendicular to the hybrids sheet calculated using GGA-RPA.

where a_H is the Bohr radius of hydrogen atom.

The e-h correlations modify dramatically the optical spectra. More precisely, in the four configurations, excitonic absorption edges are red-shifted and the spectrum profile is completely different compared to the GW-RPA spectrum with a main increase in its relative absorption intensity. Indeed, the main part of the absorption spectra is shifted back to the GGA-RPA position but with an important redistribution of the resonances due to correlations and for instance excitonic features, which are inexistent in RPA.

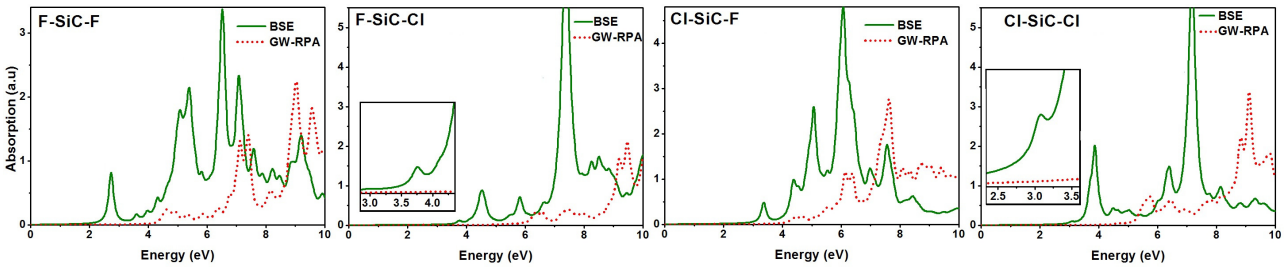

FIG. 7: Imaginary part of macroscopic dielectric function of SiC hybrid calculated using both BSE and GW-RPA.

The first absorption peak is observed at 2.73eV, 2.96eV and 3.36eV for F-SiC-F, F-SiC-Cl and Cl-SiC-F respectively. It corresponds in the three cases to optically active (bright) excitonic state. In the three halogenated structures, the strongly bound excitons result from vertical transitions between the top of valence band (degenerated) to the bottom of conduction band at Γ-point. Thus,

they are double degenerate. Their exciton binding energies, (defined as the difference between the energy of optical excitation and electronic gap), their Bohr radius and their effective mass are listed in Table 1. Notice that the exciton binding energy, corresponding to F-SiC-F, intermediates between fluorographene with 1.96eV [34] and fluorosilicene having 1.48eV [36].

The situation is different for full chlorinated SiC that is a semiconductor with indirect band gap. The first exciton observed in the optical spectrum is a dark exciton located at 3.04eV. This strongly bound excitonic state has an e-h binding energy of 1.34eV and is due to the reversion of the oscillator strength of the first active and the first inactive excitons when the light polarization changes [48]. Furthermore, the first optically active (bright) exciton emerges at 3.07eV which allowed vertical transitions from the top two valence bands to the bottom of conduction band at Γ-point. This bright exciton is characterized by a binding energy of 1.31eV and an effective mass of $0.26m_0$.

It follows full fluorination and full chlorination increase optical binding energy of pristine SiC [25].

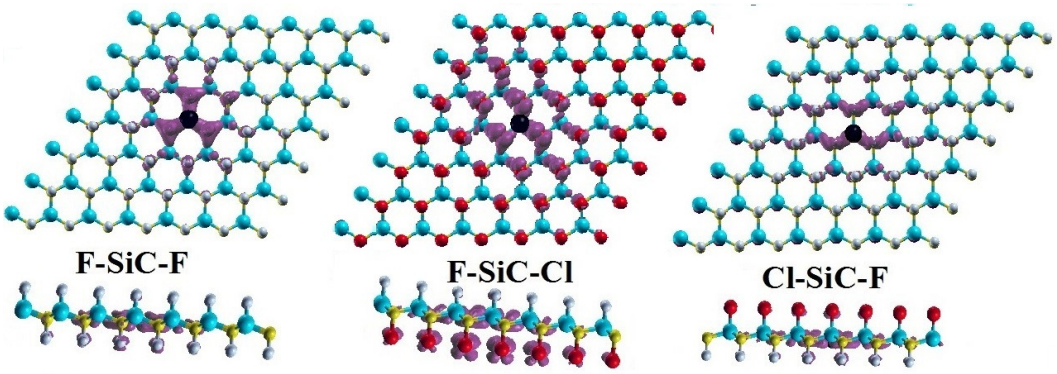

FIG. 8: Top and side view of electron probability distribution with hole position (black circle) fixed above a C atom in F-SiC-F, F-SiC-Cl and Cl-SiC-F configurations.

Figs.8 and 9 plot electron probability distribution $|\psi(r_e, r_h)|^2$ to understand correlations between excited quasi-electron and quasi-hole states in real space. The coordinate r_e refers to electron position and r_h is the position of a hole placed slightly above a Si-atom. The electron-hole amplitude $\Psi(r_e; r_h)$ is invariant to lattice vector shifts when applied simultaneously to r_e and r_h.

In F-SiC-F and F-SiC-Cl, electron charge density is more localized around the hole with small radius of 2.34$\mathring{A}$ and 2.24$\mathring{A}$ respectively compared to 3.36$\mathring{A}$ and 4.40$\mathring{A}$ obtained in Cl-SiC-Cl and Cl-SiC-F where the exciton is delocalized along the material. So, halogenation increases significantly the radius of the exciton radius of pure SiC. As shown in side view in Figs.8 and 9, charge

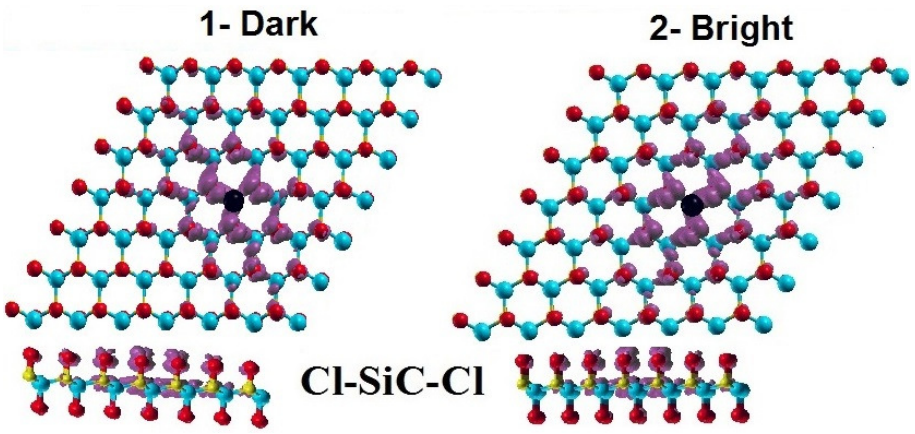

FIG. 9: Top and side view of 2D projections of electron probability distribution in Cl-SiC-Cl structure corresponding to 1- dark exciton and 2- bright exciton where the hole (black circle) is located above a C-atom

transfer occurs mainly between C- atoms and their adsorbates in the four structures. This result does not depend on the difference between electronegativities of the atoms as reported in [34] and [48]. It follows that structures where carbon is decorated with Cl, namely F-SiC-Cl and Cl-SiC-Cl, are promising candidates for possible excitonic Bose-Einstein condensation as proposed recently in the graphane case [48].

Fig. 9 shows a damping behavior for the first exciton in Cl-SiC-Cl, that is of dark-type. An identical damping nature of distribution is also observed for the bright exciton. This result reveals a strong excitonic effect. Moreover, the electron distribution associated to the first bright exciton is less localized and has a bigger radius compared to the one of fluorinated-SiC and of F-SiC-Cl. This behavior of the electron probability distribution of first active and inactive excitons is mainly due to their small binding energy of 1.31eV with respect to 1.74eV and 1.75eV obtained for F-SiC-F and F-SiC-Cl respectively. As consequence, the spatial separation of electron and hole in chlorinated SiC is the largest among the investigated materials.

Other optical quantities such as reflectivity, refractive index and electron-energy-loss function are derived from the macroscopic dielectric function $\varepsilon(\omega)$ that is calculated using GW-BSE.

At normal incidence, Fresnel reflectivity $R(\omega)$ given by:

$$R(\omega) = \left| \frac{\sqrt{\varepsilon(\omega)} - 1}{\sqrt{\varepsilon(\omega)} + 1} \right|^2 \tag{4}$$

is plotted in Fig.10 (left) for the four configurations. It is evident that these compounds behave like semiconductors since the $R(\omega)$ values are not approach to the unity towards zero energy. The zero

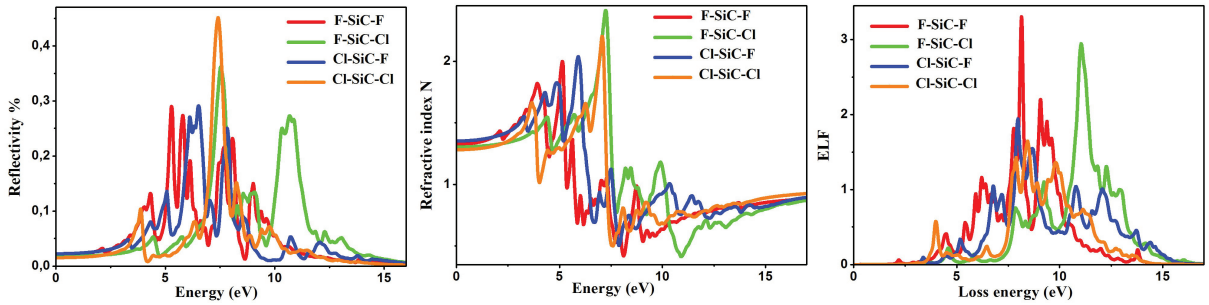

FIG. 10: (left) Reflectivity, (center) refraction index and (right) energy loss function including excitonic effects of halogenated SiC.

frequency reflectivity $R(0)$ is 0.019%, 0.017%, 0.015%, and 0.022% for of F-SiC-F, F-SiC-Cl, Cl-SiC-Cl, and Cl-SiC-F respectively. According to the reflectivity spectra these materials can be transparent in the visible region in contrast to the ultraviolet region where more reflectivity occurs.

Fig.10 (center) displays the real part of the refractive index N given by $N = n_+ + in_-$ where n_+ and n_- are refractive and extinction indexes calculated as follows:

$$n_\pm(\omega) = \sqrt{\frac{1}{2}\left(\sqrt{\Re\varepsilon(\omega)^2 + \Im\varepsilon(\omega)^2} \pm \Re\varepsilon(\omega)\right)}. \tag{5}$$

It is found that the static refraction index at zero energy takes the value of 1.32, 1.30, 1.28 and 1.35 for F-SiC-F, F-SiC-Cl, Cl-SiC-Cl, and Cl-SiC-F respectively. These values are smaller than 1.48 calculated for silicon-doped graphene [49]. In all configurations, the corresponding refraction index is minimum where absorption is maximum. Moreover, it is obvious that the obtained values are inversely proportional to the energy of direct band gap.

Finally, Fig.10 (right) presents energy-loss spectrum $L(\omega)$, another important optical characteristic that describes the energy loss of a fast electron crossing the material. It is shown that the plasmon peak occurs at 8.20 eV, 11.26eV, 8.44eV, and 7.97 eV for F-SiC-F, F-SiC-Cl, Cl-SiC-Cl, and Cl-SiC-F respectively which corresponds to a rapid decrease of reflectance in agreement with Fig.10 (left). Moreover, the collective excitation is the point of transition from the metallic to dielectric property as each material exhibits dielectric behavior above the plasmon frequency in contrast to the metallic behavior below the plasmon frequency. Notice also that the direct band gap correlates with the plasmon frequency.

IV. CONCLUSION

In summary, we have studied structural, electronic and optical properties of four halogenated SiC conformers, namely F-SiC-F, Cl-SiC-Cl, F-SiC-Cl, and Cl-SiC-F. Phonon dispersion and binding energies reveal that all the structures are stable which imply their possible fabrication and realization in laboratory. Whereas GGA-DFT calculations show that halogenation causes gap energy of SiC to decrease with respect to the pristine case, GW calculations give larger band gaps for SiC halides. The band gap is indirect in Cl-SiC-Cl and direct at Γ in the three other configurations. The resulting absorption spectra demonstrate substantial redshifts and enhancement of absorption peaks compared to the calculated spectra neglecting excitonic effects. Except Cl-SiC-F that exhibits an exciton binding energy rather similar to that of pristine SiC, F-SiC-F, Cl-SiC-Cl and F-SiC-Cl structures have huge binding energy. The strong excitonic effect in halogenated SiC makes these materials desirable for opto-electronics applications. Moreover, the charge transfer from carbon to chlorine in F-SiC-Cl and full chlorinated SiC suggest them as promising candidates for the Bose-Einstein condensation [48]. The direct controllable band gaps and the high binding energies make these materials suitable for optoelctronic applications such as, solar cell, LED, and batteries while their lower refractive index make them promising for applications in anti-reflection coatings and high-reflective systems.

Acknowledgements

L. B. Drissi and F. Z. Ramadan would like to acknowledge financial support from the Centre National pour la Recherche Scientifique et Technique (CNRST)-Morocco. L. B. Drissi and S. Lounis thank the Arab-German Young academy of Sciences and Humanities (AGYA) and the BMBF for partial funding.

[1] K.S. Novoselov, A.K. Geim, S.V. Morozov, D. Jiang , M.I. Katsnelson, I.V Grigorieva, et al. Two-dimensional gas of massless Dirac fermions in graphene. Nature **438** (7065) (2005) pp 197-200.

[2] K. S. Novoselov, A. K. Geim, S. V. Morozov, D. Jiang, Y. Zhang, S. V. Dubonos, et al. Electric field effect in atomically thin carbon films. Science **306** (5696) (2004) pp 666-669.

[3] A. B. Kuzmenko, E. van Heumen, F. Carbone and D. van der Marel. Universal optical conductance of graphite. Physical Review Letters **100** (11) (2008) pp 117401.

[4] F. Bonaccorso, Z. Sun, T. Hasan, and A.C. Ferrari. Graphene photonics and optoelectronics. Nature photonics, **4** (9) (2010) pp 611-622.

[5] R. R. Nair, P. Blake, A. N. Grigorenko, K. S. Novoselov, T. J. Booth, T. Stauber,et al. Fine structure constant defines visual transparency of graphene. Science **320** (5881) (2008) pp 1308-1308.

[6] T.H Han, Y. Lee, M.R. Choi, S.H. Woo, S.H. Bae, B.H Hong, et al. Extremely efficient flexible organic light-emitting diodes with modified graphene anode. Nature Photonics **6** (2) (2012) pp 105-110.

[7] D. R. Dreyer, S. Park, C. W. Bielawski, and R. S. Ruoff. The chemistry of graphene oxide. Chemical Society Reviews. **39** (1) (2010) pp 228-240

[8] D. C. Elias, R. R. Nair, T. M. G. Mohiuddin, S. V. Morozov, P. Blake, M. P. Halsall,et al. Control of graphene's properties by reversible hydrogenation: evidence for graphane Science **323** (5914) (2009) pp 610-613.

[9] R. Zboril, F. Karlicky, A. B. Bourlinos, T. A. Steriotis, A. K. Stubos, V. Georgakilas,et al. Graphene fluoride: a stable stoichiometric graphene derivative and its chemical conversion to graphene Small **6**, 2885 (24) (2010) pp 2885-2891.

[10] B. Li, L. Zhou, D. Wu, H. L. Peng, K. Yan, Y. Zhou, et al. Photochemical chlorination of graphene. ACS Nano **5** (7) (2011) pp 5957-5961.

[11] P. V. Medeiros, A. J. Mascarenhas, F. de Brito Mota, and C. M. C de Castilho. A DFT study of halogen atoms adsorbed on graphene layers Nanotechnology, **21** 485701 (48) (2010) pp 485701.

[12] F. Karlický, R. Zbořil, and M. Otyepka. Band gaps and structural properties of graphene halides and their derivates: A hybrid functional study with localized orbital basis sets. The Journal of chemical physics, **137** (3) (2012) 034709.

[13] S. W. Chu, S. J. Baek, D. C. Kim, S. Seo, J. S. Kim, and Y. W. Park. Charge transport in graphene doped with diatomic halogen molecules (I 2, Br 2) near Dirac point. Synthetic Metals. Synth. Met. **162** 1689 (17) (2012) pp 1689-1693.

[14] D. W. Boukhvalov and M. I. Katsnelson. Chemical functionalization of graphene. J. Phys.: Condens. Matter **21** (34) (2009) pp 344205.

[15] P. Vogt, P. De Padova, C. Quaresima, J. Avila, E. Frantzeskakis, M. C. Asensio, et al. Silicene: compelling experimental evidence for graphenelike two-dimensional silicon. Phys. Rev. Lett. **108** (15) (2012) pp 15550

[16] M. Houssa, A. Dimoulas, and A. Molle. Silicene: a review of recent experimental and theoretical investigations. J. of Phys.: Condens. Matter **27** (25) (2015) pp 253002.

[17] W. Li, S. Sheng, J. Chen, P. Cheng, L. Chen, and K. Wu. Ordered chlorinated monolayer silicene structures Phys. Rev. B, **93**, (15) (2016) pp 155410.

[18] N. Gao, W. T. Zheng, and Q. Jiang. Density functional theory calculations for two-dimensional silicene with halogen functionalization. Physical Chemistry Chemical Physics **14** (1) (2012) pp 257-261.

[19] W. B. Zhang, Z. B. Song Z B and L. M. Dou. The tunable electronic structure and mechanical properties of halogenated silicene: a first-principles study. J. Mater. Chem. C **3** 3087 (13) (2015) pp 3087-3094.

[20] S.Chabi, H. Chang, Y. Xia, and Y. Zhu. From graphene to silicon carbide: ultrathin silicon carbide flakes. Nanotechnology, **27** (7) (2016) pp 075602.

[21] H. Sahin, S. Cahangirov, M. Topsakal, E. Bekaroglu, E. Akturk, R. T. Senger, et al. Monolayer honeycomb structures of group-IV elements and III-V binary compounds: First-principles calculations. Phys. Rev. B **80** (15) (2009) pp 155453.

[22] E. Bekaroglu, M. Topsakal, S. Cahangirov, and S. Ciraci. First-principles study of defects and adatoms in silicon carbide honeycomb structures. Physical Review B **81 (7)** (2010) pp 075433

[23] L. B. Drissi, E. H. Saidi, M. Bousmina, and O. Fassi-Fehri. DFT investigations of the hydrogenation effect on silicene/graphene hybrids. Journal of Physics: C. Condensed Matter **24** (48) (2012) pp 485502.

[24] Z. Shi, Z. Zhang, A. Kutana, and B. I. Yakobson. Predicting two-dimensional silicon carbide monolayers. ACS nano **9** (10) (2015) pp 9802-9809.

[25] L. B. Drissi, and F.Z Ramadan. Many body effects study of electronic & optical properties of silicene–graphene hybrid. Physica E: Low-dimensional Systems and Nanostructures **68** (2015) pp 38-41.

[26] S. S Lin. Light-emitting two-dimensional ultrathin silicon carbide. The Journal of Physical Chemistry C **116** (6) (2012) pp 3951-3955.

[27] G. D. Scholes, and G. Rumbles. Excitons in nanoscale systems. Nature Materials, **5** (9) (2006) pp 683-696.

[28] E. Poem, Y. Kodriano, C. Tradonsky, N. H. Lindner, B. D. Gerardot, and P. M. Petroff. Accessing the dark exciton with light. Nature Phys. **6** (12) (2010) pp 993-997.

[29] L. B. Drissi, and K. Sadki. Elastic properties and sound velocities of silicane/graphane hybrids. Mechanics of Materials. **89** (2015) pp 151-158.

[30] L.B. Drissi, F.Z. Ramadan, E.H. Saidi, E., M. Bousmina, and O. Fassi-Fehri. Fluorination Effects on Electronic and Magnetic Properties of Silicene/Graphene Hybrids. Journal of the Physical Society of Japan, pp 104711.

[31] M. Rohlfing and S. G. Louie. Excitons and optical spectrum of the Si (111)-(2× 1) surface. Phys. Rev. Lett. **83**. (4) (1999) 856.

[32] P. E. Trevisanutto, M. Holzmann, M. Côté and V. Olevano. Ab initio high-energy excitonic effects in graphite and graphene. Phys. Rev. B **81 (**12**)** (2010) pp 121405

[33] M. Rohlfing, and S.G. Louie. Electron-hole excitations and optical spectra from first principles. Phys. Rev. B **62** (8) (2000) pp 4927.

[34] W. Wei and T. Jacob. Electronic and optical properties of fluorinated graphene: A many-body perturbation theory study. Phys. Rev. B **87** (11) (2013) pp 115431.

[35] F. KarlickyÌ, and M. Otyepka. Band gaps and optical spectra of chlorographene, fluorographene and graphane from G_0W_0, GW_0 and GW calculations on top of PBE and HSE06 orbitals. Journal of chemical theory and computation **9** (9) (2013) pp 4155-4164 .

[36] W. Wei and T. Jacob. Strong many-body effects in silicene-based structures. Physical Review B, **8**8 (4) pp 045203.

[37] P. Giannozzi, S. Baroni, N. Bonini, M. Calandra, R. Car, C. Cavazzoni, et al. QUANTUM ESPRESSO: a modular and open-source software project for quantum simulations of materials. J. Phys.: Condens. Matter. **21** (39) (2009) pp 395502.

[38] J.P. Perdew, K. Burke, and M. Ernzerhof. Generalized gradient approximation made simple. Physical review letters. Phys. Rev. Lett. **77** (18) (1996) pp 3865.

[39] N. Troullier, and J. L.Martins. Efficient pseudopotentials for plane-wave calculations. Phys. Rev. B, **43** (3) (1991) pp 1993

[40] A. Marini, C. Hogan, M. Grüning and D. Varsano. Yambo: an ab initio tool for excited state calculations. Comput.Phys. Commun. **180** (8) (2009) pp 1392-1403.

[41] L. Hedin and S. Lundquist. Explicit local exchange-correlation potentials. J. Phys. C: Solid State Phys. **4 (**14**)** (1970) pp 2064.

[42] R. Ahuja, S. Auluck, J. M. Wills, M. Alouani, B. Johansson and O. Eriksson. Optical properties of graphite from first-principles calculations. Physical Review Phys. Rev. B **55 (**8**)** (1997) pp 4999.

[43] A. L. Fetter and J. D. Walecka, Quantum Theory of Many-Particle Systems, Dover, New York, (2003).

[44] G. Henkelman, A. Arnaldsson, and H. Jonsson. A fast and robust algorithm for Bader decomposition

of charge density. Comput. Mater. Sci. **36** (3) (2006) pp 354-360.

[45] O. Leenaerts, H. Peelaers, A.D. Hernandez-Nieves, B. Partoens, and F.M. Peeters. First-principles investigation of graphene fluoride and graphane. Phys. Rev. B **82** (19) (2010) pp 195436

[46] L. B. Drissi and F. Z. Ramadan. Excitonic effects in GeC hybrid: Many-body Green's function calculations. Physica E: Low-dimensional Systems and Nanostructures, **74** (2015) pp 377-381

[47] D. Lee, J. Seo, X. Zhu, J. Lee, H. J.Shin, J. M. Cole, et al. Quantum confinement-induced tunable exciton states in graphene oxide. Scientific reports **3** (2013) pp 2250.

[48] P. Cudazzo, C. Attaccalite, I. V. Tokatly and A. Rubio. Strong charge-transfer excitonic effects and the Bose-Einstein exciton condensate in graphane.Phys. Rev. Lett. **104** (22) (2010) pp 226804.

[49] M. Shahrokhi, and C. Leonard. Tuning the band gap and optical spectra of silicon-doped graphene: Many-body effects and excitonic states. Journal of Alloys and Compounds, **693** (2017) pp 1185-1196.